Boundary-Layer Meteorol
DOI 10.1007/s10546-016-0214-1

RESEARCH ARTICLE

Ground-Based Observations of the Thermodynamic and Kinematic Properties of Lake-Breeze Fronts in Southern Manitoba, Canada

Michelle Curry[1,2] · John Hanesiak[1] · Scott Kehler[1] · David M. L. Sills[3] · Neil M. Taylor[4]

Received: 27 February 2016 / Accepted: 18 October 2016

Abstract The "Effects of Lake Breezes on Weather in Manitoba" project was conducted during 6–24 July 2013 to better understand local lake-breeze characteristics. Data were collected using a variety of platforms including Doppler wind lidar, rawinsondes, Doppler radar, surface meteorological stations, and a mobile weather station. The spatial and temporal variability of thermodynamic and kinematic characteristics of lake-breeze fronts are presented for three cases. Lake-breeze frontal passages were characterized by an average increase in dew point of 2.5 °C and decrease in temperature of 0.5 °C. The lake-breeze front width varied significantly over multiple measurements and cases, ranging between 50 and 800 m. The depth of the lake-breeze circulation varied between 100 and 700 m. Vertical velocities were measured at the lake-breeze front using lidar, with upward velocities of 2–3 m s^{-1} and small downward velocities of magnitude 0.5 m s^{-1} behind the front. These observations of lake-breeze fronts in southern Manitoba contribute both to the local and broader understanding of the variability (temporally and spatially) of inland shallow lake breezes.

Keywords Atmospheric boundary layer · Lake-breeze fronts · Mesoscale circulation

✉ Michelle Curry
michelle.curry@canada.ca

1 Department of Environment and Geography & Centre for Earth Observation Science, University of Manitoba, Winnipeg, MB R3T 2N2, Canada

2 Prairie and Arctic Storm Prediction Centre, Environment and Climate Change Canada, Winnipeg, MB, Canada

3 Cloud Physics and Severe Weather Research Section, Environment and Climate Change Canada, Toronto, ON M3H 5T4, Canada

4 Applied Environmental Prediction Science, Environment and Climate Change Canada, Edmonton, AB T6B 1K5, Canada

Published online: 09 November 2016

1 Introduction

The sea/lake breeze, a type of thermally-induced mesoscale circulation, plays an important role in regulating the climate of near-shore regions (e.g. Pearce 1955; Oke 1978; Simpson 1994) and can influence the location, timing, and intensity of convective initiation and storms (Sills 1998; King et al. 2003; Azorin-Molina et al. 2009; Alexander 2012). Evidence from southern Ontario suggests that lake-breeze circulations have a large influence on tornado and thunderstorm climatology, potentially suppressing or enhancing severe thunderstorms (King et al. 2003). A number of investigations have been conducted on sea and lake breezes, particularly in the Great Lakes and Florida regions of North America (e.g. Lyons 1972; Estoque et al. 1976; Sills 1998; Laird et al. 2001; King et al. 2003; Sills et al. 2011), but few investigations have been done in other regions for comparison.

Lake-breeze circulations develop as a result of microclimatic differences, namely the horizontal pressure gradient that results from a difference in air temperature over land and water (e.g. Pearce 1955; Oke 1978). The sea/lake breezes experienced near the surface are the manifestation of the low-level portion of the circulation cell (Oke 1978); as the circulation develops, the onshore flow at the surface propagates further inland. The lake-breeze front (LBF) is the maximum inland extent of this flow and is usually characterized by a sharp change in wind direction, decrease in air temperature, increase in dew point, and enhanced lift due to the circulation and convergence of the onshore flow with the larger scale flow (Lyons 1972; Sills et al. 2011).

The first attempt to characterize LBFs in Manitoba, Canada was made by Curry et al. (2015) using radar-based analysis that showed LBFs occurring on roughly 40 % of days in the warm season months. However, there was large variability from month to month, and year to year. Their analysis also showed that while radar is useful for detecting LBFs forming around Lake Manitoba (see Fig. 1), up to half of LBFs from Lake Winnipeg were missed due to the large distance from the lakeshore to the radar. The "Effects of Lake Breezes on Weather in Manitoba" (ELBOW-MB) field project was developed to better understand the properties of lake breezes and their influence on weather in southern Manitoba. A three-week intensive observation period IOP was conducted between 6 and 24 July 2013 to collect observations for a number of LBF cases. The results from this study represent the most thorough investigation of lake breezes in Southern Manitoba to date, aiding in our understanding of the characteristics of lake breezes in the region. The results are unique in the lake-breeze literature as there have been no published results to date of mobile weather station measurements of lake-breeze circulations, and no published results of Doppler wind lidar measurements of lake breezes in Canada. As Segal et al. (1997) point out, given the large variety of lakes (in shape, size, and orientation), a thorough examination of a variety of lake types is required to provide a full understanding of the lake-breeze circulation.

The overall goal is to examine the spatial and temporal variability of the thermodynamic and kinematic characteristics of LBFs in southern Manitoba. We present three cases from the intensive observation period: two for LBFs that formed near the western shore of Lake Winnipeg, and one for a LBF near the south-eastern shore of Lake Manitoba. The study area characteristics and data collected are discussed in Sect. 2. The synoptic-scale environment and characteristics of the resulting LBFs are examined individually in Sect. 3, and then summarized and discussed in a broader context in Sect. 4.

2 Data and Methods

2.1 Study Area

Two of the largest fresh water lakes in the world are located in southern Manitoba, Canada; Lake Winnipeg (11th largest) and Lake Manitoba (33rd largest). Combined, the lakes represent an area of over 29 000 km^2 and over 2 500 km of shoreline and are generally shallow, between 7 and 12 m deep. While Lake Winnipeg has a narrow southern basin, with an irregular coastline, Lake Manitoba has a slightly wider southern basin with a rounded coastline. There is also a group of three small lakes; East, West, and North Shoal Lake (referred to hereafter as the Shoal Lakes) ranging in diameter from 3 to 6 km that are susceptible to frequent flooding resulting in a small shallow 12 km wide lake. Water temperatures for Lake Winnipeg (from an Environment and Climate Change Canada [ECCC] buoy) range from 14 °C in early June to 26 °C in August, with an average temperature in 2013 of 19 °C. This is in contrast to the Great Lakes bordering Ontario and Michigan, which are generally deeper and colder (15 °C for Lake Superior to 24 °C for Lake Erie; NOAA 2015) and cover a greater surface area.

Figure 1 shows the study region and the locations of data collection sites such as the Woodlands (referred to hereafter as XWL) Doppler Radar, including range rings from the XWL radar to 120 km (near maximum detection range for XWL in Doppler mode). As the radar beam height increases with distance from the radar, the probability of detecting LBFs decreases, and at 120 km the centre of the radar beam on a 0.5-degree scan would be approximately 2000 m above the ground, assuming a standard atmosphere. Previous research has indicated LBFs generally reach a depth of between 100 and 1000 m (Lyons 1972; Simpson 1994; Suresh 2007; Tsunematsu et al. 2009), and at 2000 m the radar beam typically overshoots the top of the LBF. Also included in Fig. 1 are the locations of the meteorological stations in the study area, including ECCC, Manitoba Agriculture, Food, and Rural Initiatives (MAFRI), and ELBOW-MB stations.

2.2 Data

Data were obtained from meteorological towers, an automated mobile meteorological observation system (AMMOS), and a mobile atmospheric research station (MARS). These data were supplemented by archived data including satellite images, upper air analyses, Doppler radar, ECCC weather stations, and MAFRI weather stations (locations shown in Fig. 1). Three LBF cases were selected for this study; two cases from Lake Winnipeg (14 and 17 July), and one case from Lake Manitoba (13 July), and selected based on the most complete data collection during ELBOW-MB.

2.2.1 Regional Data

Surface meteorological data consisted of observations from weather stations and the ECCC buoy in the south basin of Lake Winnipeg. Radar and satellite images were used to examine the evolution of LBFs for each case. The XWL radar is a 5-cm (C-Band) Doppler radar with a 10-min scan interval; images from the lowest-level (0.5 degree) Doppler reflectivity scan were found to best capture clear-air returns and boundary-associated fine lines (Wilson and Schreiber 1986). Initiation and dissipation times (first and last image where a fine line was visible, respectively), penetration distance, speed, and maximum reflectivity values along

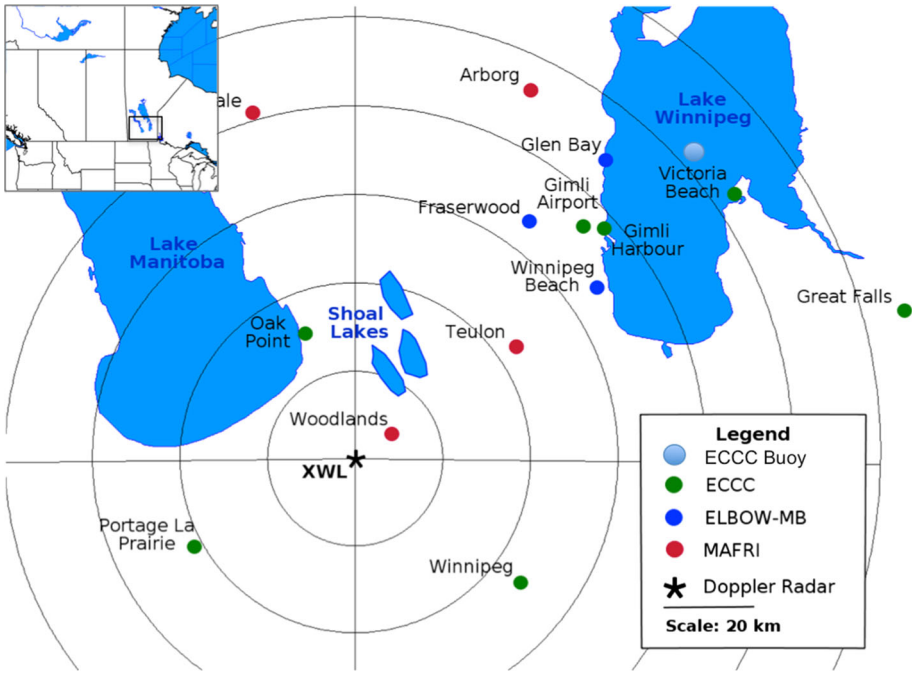

Fig. 1 The ELBOW-MB domain highlighting surface meteorological stations (*filled circles*) and the location of the Woodlands radar (*star*). The concentric circles are radar range rings at 20-km intervals

the LBF were analyzed with unified radar processor software. Visible satellite images were archived for each case from the GOES-13 satellite (4-km resolution).

Following the criteria outlined by Sills et al. (2011), these data were analyzed to determine whether a lake breeze occurred. Criteria include the presence of a fine line on radar forming near the lake and moving inland, enhanced cumulus clouds at the edge of the LBF, and a change to onshore winds at surface stations within the lake breeze. For a detailed description of the criteria used refer to Sills et al. (2011).

2.2.2 Mobile Atmospheric Research Station

The MARS was equipped with a Leosphere Windcube 70S Doppler lidar and a mobile rawinsonde unit; the lidar uses a 1.54-μm laser with a 0.1-Hz scan frequency. The maximum height of detection ranges from 100 to 2000 m above ground level (a.g.l.; depending on the number of aerosols in the lower troposphere), with a wind speed (both horizontal and vertical) accuracy of 0.3 m s^{-1} (between zero and 100 m s^{-1}), and direction accuracy of 1.5°. The MARS was deployed near the lake and left stationary to measure changes in wind direction, wind speed, and vertical velocity over time before, during, and after a LBF passage.

The rawinsonde unit was mobile during the intensive observation period with launches generally done prior to lake-breeze development and after a LBF passage to sample the lake-breeze modified airmass. Additional launches were done where possible in both airmasses to capture changes over time. The depth of each lake breeze was estimated from lake-modified airmass soundings by noting maximum depth of the onshore flow, where the depth measurement is rounded to the nearest 50 m to reflect uncertainties in the rawinsonde observations. Each case presented here had a background wind direction directed offshore in the low levels.

If the background wind direction had been directed onshore at the low levels, this method would be less effective for determining the depth of the circulation as the onshore portion of the circulation would have been embedded within the background flow.

2.2.3 Automated Mobile Meteorological Observation System

An AMMOS was used to conduct transects across the LBF, with similar instrumentation developed as part of the "Verification of the Origins of Rotation in Tornadoes Experiment" (VORTEX; Straka et al. 1995). Subsequent studies of convection and tornadogenesis including VORTEX 2 (Wurman et al. 2012) and the "Understanding Severe Thunderstorms and Alberta Boundary Layers Experiment" (UNSTABLE; Taylor et al. 2011) also used an AMMOS to investigate thermodynamic gradients across low-level boundaries. AMMOS measurements were collected as part of the "Border Air Quality and Meteorology" (BAQS-Met) project studying lake breezes in southern Ontario (Brook et al. 2013); however, to date, there have been no published results of lake-breeze front measurements using AMMOS.

The AMMOS was driven through the LBF at a constant speed, quasi-perpendicular to the LBF to limit errors in width measurements. Vehicle speed varied between transects depending on the intensity of the LBF measured on the first transect. In some cases, for a particularly sharp LBF or a fast moving LBF, the AMMOS would be kept stationary allowing the LBF to pass over the vehicle. Measurements were taken every 1 s and monitored in real time, with wind measurements corrected for the movements of the vehicle using GPS to provide true wind speed and direction. Data were collected for a minimum of 1 min at the start and end of each transect to ensure that the sensors had stabilized in the given airmass before proceeding.

The leading edge of the LBF was considered the first data point at which large and sustained changes in dew point occurred (at least 0.2 K s^{-1}) combined with a wind shift directed from offshore to onshore flow. The trailing edge of the LBF was considered the final data point at which the wind shift or dew point changes occurred and the measurements subsequently stabilized. Note that these changes did not necessarily occur simultaneously.

The latitude and longitude of the AMMOS at the start and end of the LBF transect was then used to determine the width of the front. A secondary calculation of each LBF width was made using the speed of the AMMOS and the passage time across the LBF. In all cases, the speed measurement was within 50 m of the GPS measurement. Temperature, dew point, and wind speeds were averaged from the start of the transect to the leading edge of the LBF, and from the trailing edge of the LBF to the end of the transect, to calculate average airmass characteristics on either side of the LBF. Since width calculations assume the LBF is stationary relative to the movement of the AMMOS, width estimates are rounded to the nearest 50 m in an attempt to address uncertainties in the location of the LBF. Other potential sources of error include the response rate of the humidity and wind-direction sensors and the direction of movement of the LBF relative to the AMMOS. These errors were mitigated through use of the J-tube, which provides aeration to ensure ambient air is being sampled, and the use of a fast response temperature sensor.

3 Results

3.1 13 July 2013—Lake Manitoba

The study area was under the influence of an anticyclone located to the west, and a warm front located in North Dakota moving northward; surface wind directions in the study area were

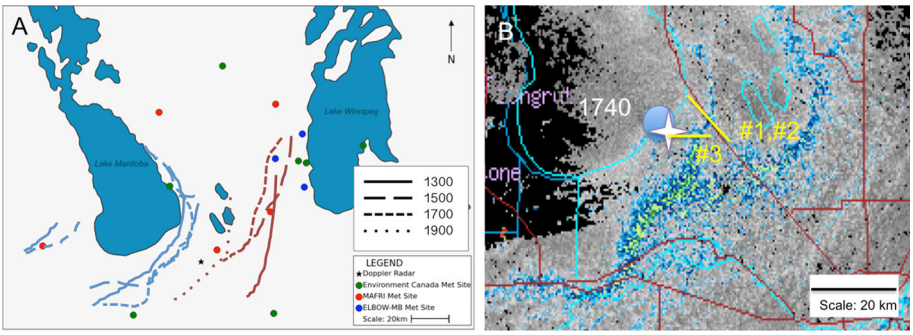

Fig. 2 LBF and observation locations for 13 July 2013: **a** shows locations of the LBF every 2 h for Lake Manitoba (*blue*) and Lake Winnipeg (*red*) with times as indicated (CDT), and **b** Doppler radar image (zoomed in to highlight the Lake Manitoba LBF) at 1700 CDT showing the sounding location (*blue dot*, with launch time indicated in CDT), MARS location (*white star*), and AMMOS transects (*yellow lines, numbered*) sampling the Lake Manitoba LBF

east to north-east, with wind speeds $< 5\,\mathrm{m\,s^{-1}}$. The ambient air temperature in the study region surrounding Lake Manitoba was 28 °C. Water temperature measurements are not available for Lake Manitoba, however, given similar lake characteristics the Lake Winnipeg buoy was used as a proxy for this case; water temperature was 26 °C, and air temperature at the buoy was 25 °C. LBF initiation was first noted on Doppler radar at 1100 CDT (central daylight time), and persisted until 2020 CDT, with LBF penetration noted to approximately 25 km inland at maximum extent (see Fig. 2a).

The MARS was deployed on the south shore of Lake Manitoba and a rawinsonde released at 1740 CDT (location indicated in Fig. 2b, profile Fig. 3). As the south shore of Lake Manitoba is oriented south-west to north-east, the wind velocity (V') components were transformed such that V' represents a north-west to south-east flow perpendicular to the shoreline. A negative V' value indicates onshore flow. The data indicate onshore flow with a reduction in temperature and increase in dew point (relative to the airmass aloft) to 250 m (all heights reported above ground level unless otherwise noted). The synoptic wind direction at a height of 1.5 km was from the south (offshore), as opposed to the north-east flow at the surface. Therefore, the return flow, if present, was embedded within the background flow for this case.

The lidar was also deployed south of Lake Manitoba (see Fig. 2b), however data collection began after the LBF had passed and are not shown here. Data were collected between 1755 and 1900 CDT for the depth of the lake-breeze circulation behind the front. Generally, negative (downward) vertical velocities of $-0.5\,\mathrm{m\,s^{-1}}$ were recorded, with occasional values as high as $-2.0\,\mathrm{m\,s^{-1}}$ and no strong positive vertical velocities recorded. This follows the conceptual model for a lake breeze as the circulation behind the LBF is associated with downward motion and an inversion at the transition between the onshore marine air and the residual layer and return flow aloft. The depth of the onshore flow varied between 300 and 400 m over a short time period (5–10 min), noting that these depth measurements are comparable with those from the rawinsonde profile.

Three transects of the LBF were obtained using the AMMOS (see Table 1). The first two transects were along a line oriented north-west to south-east from the south-east corner of the lake (shown in Fig. 2b) between 1616 and 1635 CDT, and 1649 and 1959 CDT, respectively. The third transect was taken south of the lake, oriented east to west, between 1709 and 1728 CDT (Fig. 4). This was the only transect used herein where the direction of motion of the AMMOS is not perpendicular to the LBF. A trigonometric correction was applied to the width

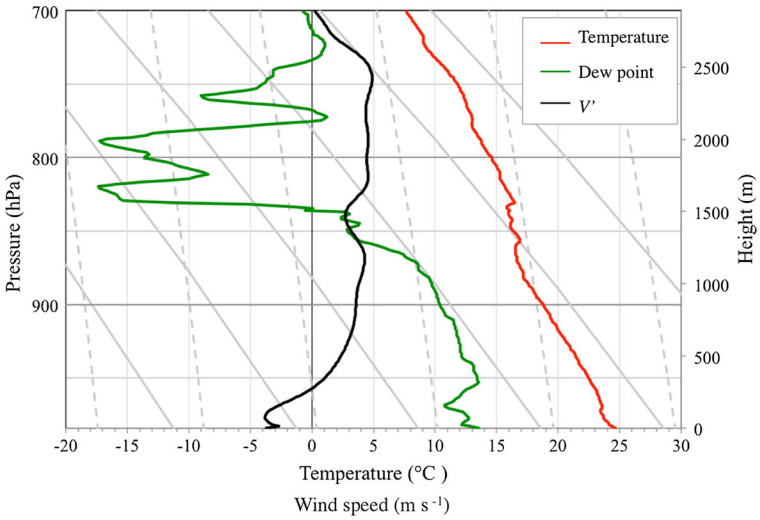

Fig. 3 Plot of sounding data for 1740 CDT 13 July 2013. Wind components were transformed to be perpendicular to the LBF, and the V' wind component (m s^{-1}), temperature (°C), and dew point (°C) plotted. Note that a negative V' value corresponds to a north-westerly wind direction, which is an onshore flow. Dry adiabats are plotted every 10 °C for reference

Table 1 AMMOS transects of Lake Manitoba LBF for 13 July 2015

#	Time start (CDT)	Time finish (CDT)	Direction travelled	Width of LBF (m)	Temperature difference (°C)	Dewpoint difference (°C)	Wind-speed difference (m s^{-1})
1	1616	1635	North-west	500	−0.3	2.6	0.8
2	1649	1659	South-east	800	−0.3	2.6	0.8
3	1709	1728	West	450	−0.4	2.6	1.3
		Mean		600	−0.3	2.6	1.0

Differences are calculated as the land to marine transition. Transect numbers correspond to transects marked in Fig. 2b

of the LBF to account for the relative angle of motion. The thermodynamic characteristics of the land- and lake-modified airmasses, respectively, were similar between the three transects. The wind direction within the lake-modified airmass was generally northerly (onshore) while the direction within the land airmass was easterly creating a zone of convergence at the LBF. The average width of the LBF over the three transects was 600 m; air temperature was 0.4 °C lower, dew point 2.6 °C higher, and wind speed 1 m s^{-1} greater, on average, within the lake airmass.

3.2 14 July 2013—Lake Winnipeg

An anticyclone located to the west of the study area resulted in wind direction generally from the north to north-west, with wind speed of 4 m s^{-1} increasing to 5–10 m s^{-1} in the afternoon. The ambient air temperature in southern Manitoba ranged from 24 to 26 °C, while the Lake Winnipeg water temperature reached 21 °C. Lake-breeze front development was

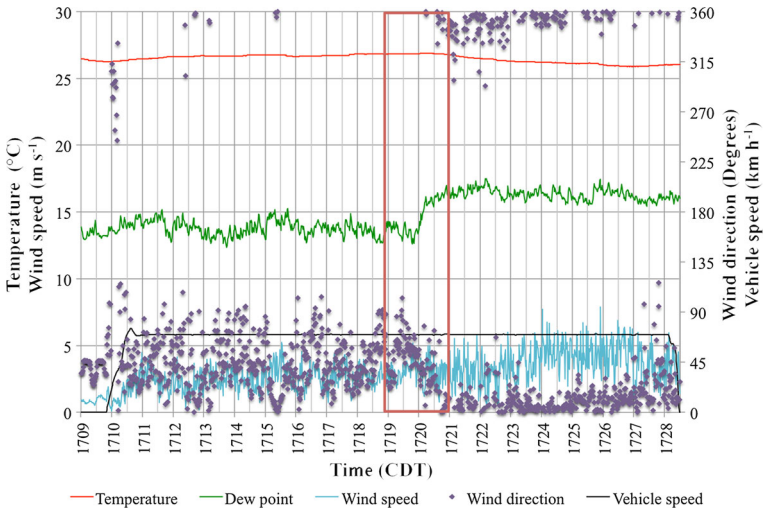

Fig. 4 AMMOS transect number 3 of Lake Manitoba LBF for 1709–1728 CDT 13 July 2013. Sampling of the LBF is outlined in *red*. *Red line* indicates temperature (°C), *green line* dew point (°C), *blue line* wind speed (m s^{-1}), *black line* vehicle speed (km h^{-1}), and *purple dots* wind direction (degrees)

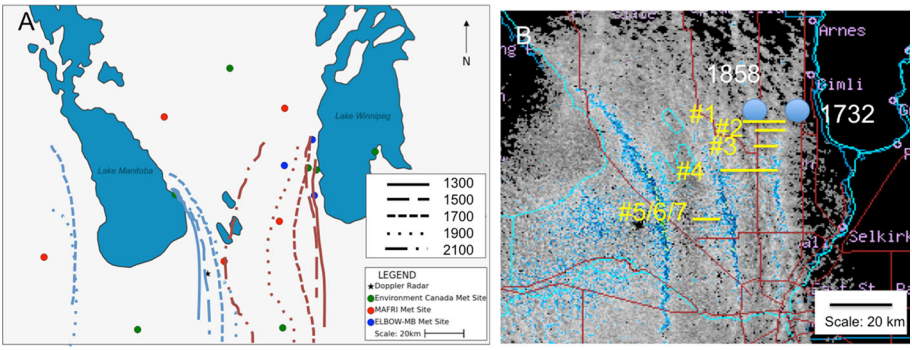

Fig. 5 LBF and observation locations for 14 July 2013: **a** shows the locations of the LBF every 2 h for Lake Manitoba (*blue*) and Lake Winnipeg (*red*) with times indicated (CDT), and **b** Doppler radar image (zoomed to highlight LBFs from Lake Winnipeg and Shoal Lakes) at 1700 CDT showing the sounding locations (*blue dots*, launch time indicated in CDT), and AMMOS transects (*yellow lines, numbered*) of Lake Winnipeg LBF

first noted on Doppler radar at 1100 CDT and persisted until 2140 CDT. The LBF penetrated 110 km from the west shore of Lake Winnipeg passing the Shoal Lakes and merging with the Lake Manitoba LBF (see Fig. 5a).

The MARS was fully mobile during this case with no lidar measurements taken. Two rawinsondes were launched into the lake-modified airmass, one at 1732 CDT from Winnipeg Beach, and another at 1858 CDT 15 km to the west (location shown in Fig. 5b). The first profile showed onshore winds (negative U component or easterly wind) to a depth of 400 m, with a lower temperature to the same depth (shown in Fig. 6). Higher dew points were confined to the lowest 100 m. The second profile showed an increased depth of onshore flow to 600 m (200 m higher than the first profile), with thermodynamic changes occurring to roughly the same depth (within 100 m). The first sounding recorded slightly stronger offshore winds

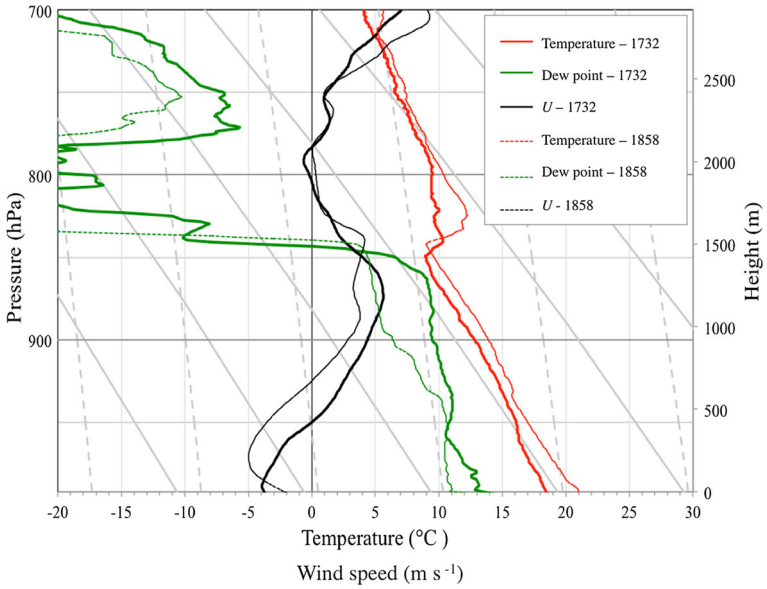

Fig. 6 Plot of the sounding data for Lake Winnipeg LBF at 1732 and 1858 CDT 14 July 2013. *U* wind component (east-west wind directions; m s^{-1}), temperature (°C), and dew point (°C) plotted. Note a negative *U* value corresponds to an easterly wind, which is an onshore flow. Dry adiabats are plotted every 10 °C for reference

(8 m s^{-1} on average) between 1000 and 1500 m compared to the second sounding (6 m s^{-1}). As this sounding was taken directly near the lakeshore, it is possible that this increase in wind speed is a result of the return flow of the lake-breeze circulation, providing an additive effect on the background wind speed as both flows are directed offshore. The second sounding also shows a localized increase in wind speed aloft, but not as strong. The wind speed decreases by less than 2 m s^{-1} for both soundings directly above this height as well, further suggesting the presence of a return flow aloft.

Four AMMOS transects of the Lake Winnipeg LBF were analyzed for this case (location shown in Fig. 5b), with all four transects located on roads oriented east to west, perpendicular to the LBF. The thermodynamic differences between the lake- and land- modified airmasses were similar between the four transects, with an average temperature 0.5 °C lower, dew point 2.3 °C higher, and wind speed 0.7 m s^{-1} greater in the lake-modified airmass. The average measured width of the LBF was 350; 200 m narrower on average than the first case.

Three additional transects were analyzed showing the Lake Winnipeg LBF merging with the Shoal Lake LBF (shown in Fig. 5b, transects 5–7 in Table 2). After merging, only the Lake Winnipeg LBF was visible on radar, with the timing and location corresponding to when the collision was noted in the AMMOS. Pre-merge measurements were taken while leaving the AMMOS stationary, letting the LBF pass over the vehicle (1908 CDT, outlined in red on Fig. 7). The width of the LBF was calculated by estimating the speed of the LBF using the radar and the time for the LBF to pass the AMMOS. Between 1910 and 1920 CDT, Doppler radar showed that the Lake Winnipeg LBF merged with the Shoal Lakes LBF. The second transect was taken shortly after the collision (outlined in green in Fig. 7); the width of the LBF was slightly wider than earlier in the day, at 600 m, and there was almost no change in moisture or temperature across the LBF as both airmasses sampled were modified

Table 2 AMMOS transects of the Lake Winnipeg LBF on 14 July 2013

#	Time start (CDT)	Time finish (CDT)	Direction travelled	Width of LBF (m)	Temperature difference (°C)	Dew point difference (°C)	Wind speed difference (m s^{-1})
1	1544	1556	East	350	−0.3	2.3	0.5
2	1559	1610	West	400	−0.7	2.9	1.2
3	1642	1650	East	250	−0.5	2.0	0.3
4	1706	1726	West	350	−0.6	2.1	0.8
		Mean		350	−0.5	2.3	0.7
5	1900	1910	NA	200	−0.4	3.4	−0.5
6	1912	1922	West	600	0.1	0.6	1.2
7	1924	1930	East	200	0.2	0.1	1.4

The final three transects were taken directly before and after a merging between the Lake Winnipeg LBF and the Shoal Lakes LBF. Differences are calculated as the land to marine transition. Transect numbers correspond to locations in Fig. 5b

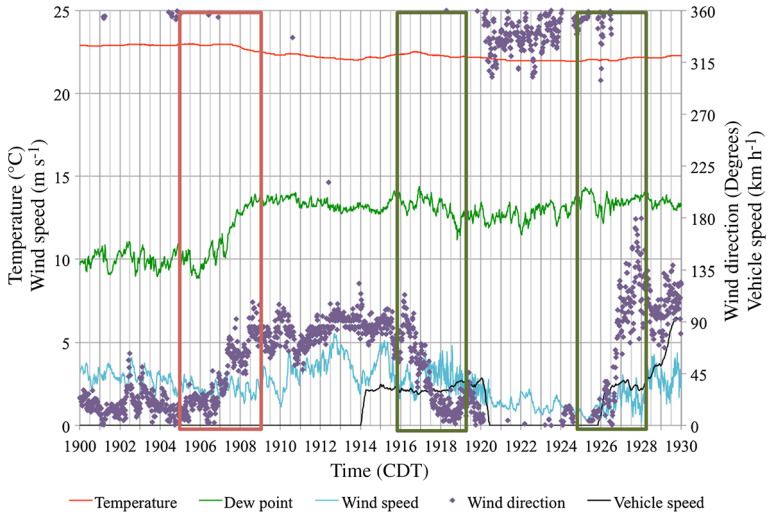

Fig. 7 AMMOS transect for 1900–1930 CDT on 14 July 2013. Sampling of the LBFs is outlined; Lake Winnipeg (*red*) and Lake Winnipeg–Shoal Lakes LBF collision (*green*). *Red line* indicates temperature (°C), *green line* dew point (°C), *blue line* wind speed (m s^{-1}), *black line* vehicle speed (km h^{-1}), and *purple dots* wind direction (degrees)

by lake-breeze circulations. The wind speed was the only significant difference, with wind speeds on the Lake Winnipeg side of the LBF being 1.4 m s^{-1} greater than those on the Shoal Lakes side. Wind direction also briefly switched to north-north-west at 1920 before switching back to east at 1927 CDT, as seen in Fig. 7 when the AMMOS crossed the boundary again.

3.3 17 July 2013—Lake Winnipeg

An anticyclone located over the Manitoba–Saskatchewan border to the west of the study region resulted in west to north-west wind directions near the surface with wind speeds of

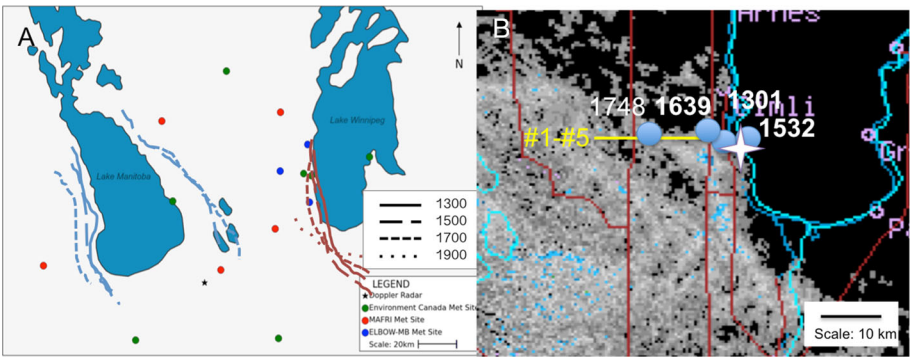

Fig. 8 LBF and observation locations for 17 July 2013: **a** shows the locations of the LBF every 2 h for Lake Manitoba (*blue*) and Lake Winnipeg (*red*) with times indicated (CDT), and **b** Doppler radar image (zoomed to highlight Lake Winnipeg LBF) at 1700 CDT showing the sounding locations (*blue dots*, launch times indicated in white in CDT), MARS location (*white star*), and AMMOS transects (along the *yellow line*) of Lake Winnipeg LBF

1–2 m s^{-1}. The ambient air temperature reached 25–30 °C at stations surrounding Lake Winnipeg, while the Lake Winnipeg water temperature reached 24 °C. LBF development was first noted on Doppler radar at 1250 CDT and persisted until 1820 CDT, penetrating 20 km inland (see Fig. 8a). An area of cirrus cloud (not shown) moved across the study region between 1400 and 1820 CDT resulting in the LBF quickly dissipating.

The lidar was deployed 1 km inland from the lakeshore (shown in Fig. 8b), while the MARS was fully mobile. Four rawinsondes were released; one before the LBF formed, two behind the LBF, and one later in the afternoon ahead of the LBF. All locations are shown in Fig. 8a. The first profile (Fig. 9a), taken at 1301 CDT, showed a well-mixed planetary boundary layer to 1500 m, and 3 m s^{-1} westerly winds. The second profile (Fig. 9a), taken at 1532 CDT, showed a wind shift to onshore flow, and thermodynamic changes up to 600 m, 150 m higher than the height of the wind shift. The third profile (Fig. 9b), taken at 1939 CDT showed similar kinematic and thermodynamic changes, with the depth of the lake-breeze circulation increasing to 700 m. As with the second profile, the thermodynamic changes were evident at heights greater than the height of the wind shift, this time to 1000 m. The final rawinsonde (Fig. 9b) was released at 1748 CDT ahead of the dissipating LBF showing a well-mixed planetary boundary layer to 1800 m. Both lake-modified soundings also showed a potential return flow aloft, marked by a localized increase in wind speed, between 1000 and 1500 m.

Lidar measurements were taken between 1420 and 1730 CDT, with the passage of the LBF at the lidar occurring at 1431 CDT (shown in Fig. 10). Prior to the LBF passage, vertical velocities ranged from 0.5 to −1.0 m s^{-1}. These initial areas of positive and negative vertical velocities are attributed to convective mixing in the planetary boundary layer. Surface winds were west to north-westerly at 4.0 m s^{-1} just prior to the LBF passage, with gusts to 10 m s^{-1}, also attributed to thermal updrafts and mixing within the planetary boundary layer.

At 1427 CDT, easterly flow and a brief increase in vertical velocities were noted, before the low-level wind direction changed back to an offshore flow. This pulsing nature of the LBF progression was noted on a number of days during the intensive observation period, with the LBF moving onshore only a few hundred metres before retreating offshore again. This appears to have happened twice before continuous onshore flow began at 1433 CDT. The zero contour for the U component of the wind velocity was included on Fig. 10 to better

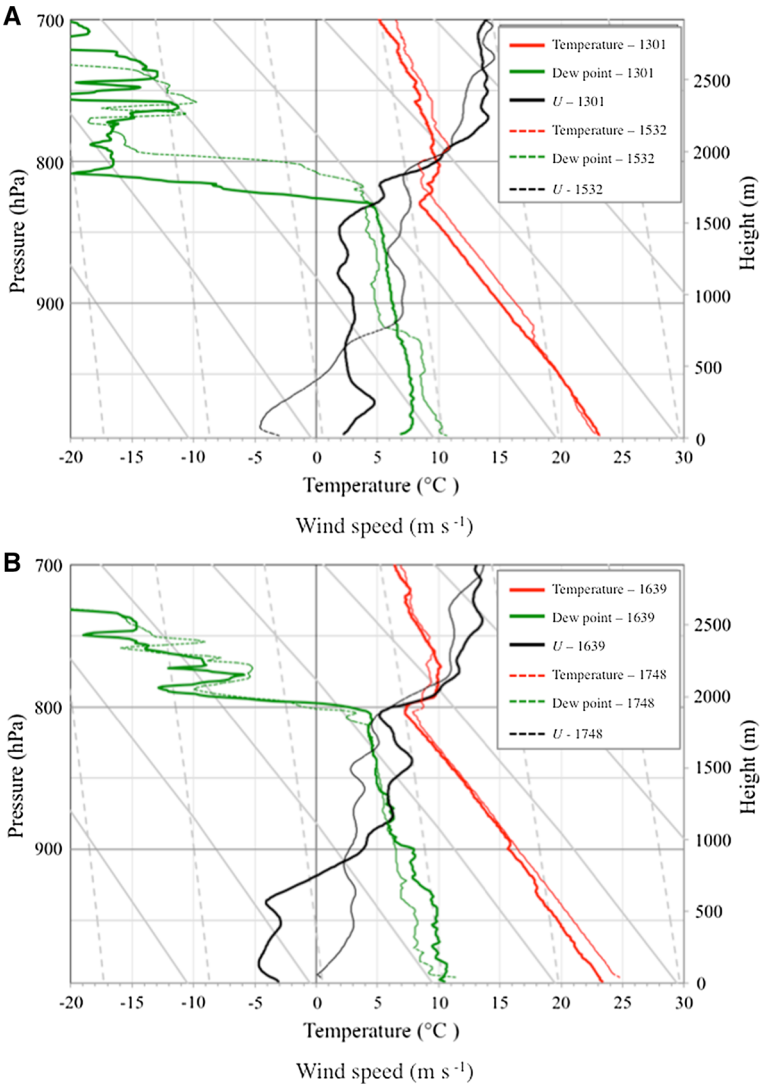

Fig. 9 Plot of sounding data for the Lake Winnipeg LBF for **a** 1301 (land) and 1532 CDT (lake) 17 July 2013, and **b** 1639 (lake) and 1748 CDT (land) 17 July 2013. *U* wind component (east-west wind directions), temperature (°C), and dew point (°C) plotted. Dry adiabats are plotted every 10 °C for reference. A negative *U* value corresponds to an easterly wind direction, which is an onshore flow

delineate the onshore flow. While there is an initial lobe of onshore flow, the general shape of the flow is more of a wedge shape, with the depth of the lake-breeze circulation increasing with time over the course of the observations. This corresponded to a rather broad area of positive vertical velocities (1.0–1.5 m s^{-1}) near the LBF that reached much higher than the onshore flow. The most likely cause of this is that the LBF forced a thermal updraft aloft as the front progressed inland. Similar to the first case, the depth of the onshore flow did not remain consistent over the life of the lake breeze, ranging from 300 to 600 m, in agreement with the values from the rawinsonde wind profiles. Once the LBF passage occurred, large areas of

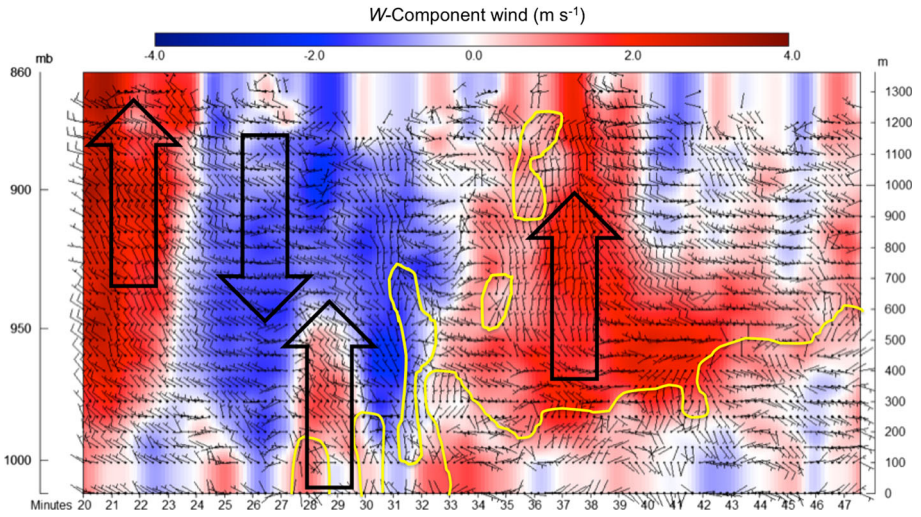

Fig. 10 Doppler lidar wind observations for Lake Winnipeg LBF for 1420–1450 CDT 17 July 2013. Time is in minutes on the horizontal axis. Wind barbs are horizontal wind speed (half barb is 2.5 m s^{-1}, full barb is 5.0 m s^{-1}). Vertical velocity (m s^{-1}) is *shaded with blue* (*red*) indicating descent (ascent), with large areas of ascent and decent marked by *arrows*. The *yellow line* delineates separation of onshore and offshore flow (zero value *U* component). Values above 850 hPa and below 1000 hPa are interpolated

positive vertical velocity were no longer present (not shown); likely a result of subsidence in the cooler marine air behind the LBF.

Five AMMOS transects were selected for this case (listed in Table 3), with all transects along one road oriented east to west, perpendicular to the lakeshore and LBF. The first transect was taken between 1445 and 1450 CDT, and the final transect was taken just before the LBF dissipated, between 1722 and 1730 CDT. Doppler radar fine line returns were quite weak on this day (see Fig. 8b), however, the locations where it was possible to discern a faint fine line return corresponded with where LBF locations were noted using AMMOS data.

While the absolute thermodynamic differences between the lake- and land-modified airmasses were similar to the previous two cases, there was more variation between transects for this case when compared to the others. The average temperature difference was 0.5 °C lower in the lake-modified airmass, with a range of −0.9 to 0.2 °C (higher than the land-modified airmass). The average dew point was 2.4 °C higher in the lake-modified airmass, with a range of 0.4–4.6 °C. The width of the LBF over the five transects ranged from 50 to 400 m, with an average width of 200 m, similar to the second case. The wind speed was also 0.5 m s^{-1} greater on average within the lake-modified airmass and from the south-east, as compared to west in the land-modified airmass, creating an area of convergence at the front. The second transect, with a LBF width measuring 50 m, was the sharpest LBF measured during the intensive observation period (see Fig. 11). The initial transects showed a more narrow LBF, however, as the afternoon progressed and the LBF moved inland, subsequent transects showed a wider LBF, with less noticeable changes in temperature, moisture, and wind. This follows past studies of LBFs (e.g. Lyons 1972), which showed that the lake airmass becomes modified by the land surface as the LBF moves inland, reducing the difference between the lake and land airmasses.

Table 3 List of AMMOS transects of Lake Winnipeg LBF for 17 July 2013

#	Time start (CDT)	Time finish (CDT)	Direction travelled	Width of LBF (m)	Temperature difference (°C)	Dew point difference (°C)	Wind-speed difference (m s^{-1})
1	1445	1451	West	200	−0.9	4.6	0.6
2	1608	1616	East	50	−0.8	3.8	1.5
3	1617	1626	West	100	−0.9	3.0	−0.6
4	1644	1651	West	300	−0.3	1.1	1.1
5	1822	1830	East	400	0.2	0.4	−0.1
		Mean		200	−0.5	2.4	0.5

Differences are calculated as the land to marine transition. Transect numbers correspond to locations in Fig. 8b

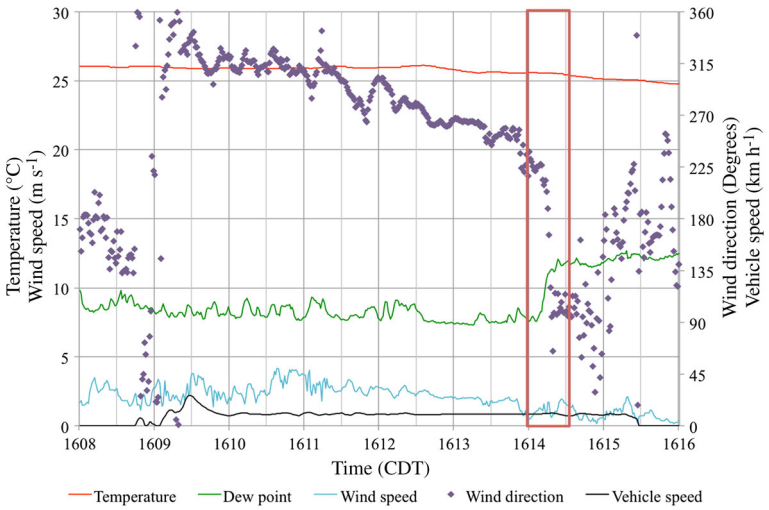

Fig. 11 AMMOS transect of Lake Winnipeg LBF for 1608–1616 CDT 17 July 2013. Sampling of the LBF is outlined in *red*. *Red line* indicates temperature (°C), *green line* dew point (°C), *blue line* wind speed (m s^{-1}), *black line* vehicle speed (km h^{-1}), and *purple dots* wind direction (degrees)

4 Summary

Information on the fine-scale structure of lake breezes in the southern Manitoba region has been provided by using a range of datasets including surface observations, Doppler radar, and in situ measurements including AMMOS, rawinsonde, and lidar wind profiles for three cases. A number of recent studies have incorporated similar observations of sea and lake breezes to calculate LBF (or sea-breeze front) depth, circulation depth behind the LBF, vertical velocities at the LBF, and kinematic characteristics within the lake-breeze circulation (e.g. Tsunematsu et al. 2009; Asefi-Najafabady et al. 2010; Iwai et al. 2011; Sills et al. 2011). A summary of our results in relation to previous studies is provided in Table 4. The results fall within the spectrum of previous studies, however, our findings indicate a much narrower zone of convergence, and also a shallower onshore portion of the lake-breeze circulation. These differences may have resulted from using high-resolution data as opposed to those used in

Table 4 Summary of the results from this study to other studies

Study	Wind speed change ($m\ s^{-1}$)	Lake-breeze depth (m)	Vertical velocity ($m\ s^{-1}$)	LBF width (m)
This study	1.0	100–600	2–3	350–650
Asefi-Najafabady et al. (2010)	2–3	1500	1.5	
Iwai et al. (2011) (sea breeze)	1.5	2000 (front) 500	5	500
Lyons (1972)		100–1000	1	1000–2000
Stull (1988) (sea breeze)		2× circulation depth at front 100–500	0.5–2.5	1000–2000
Tsunematsu et al. (2009) (sea breeze)		100–1000		
Crosman and Horel (2012)[a]		900 (front) 600		

Note that lake-breeze depths are provided for both the circulation depth and the LBF depth (or SBF depth where sea-breeze results are indicated)
[a] The results of Crosman and Horel (2012) are from a modelling study

past studies, and also differences in the size of the lake in question. As well, the measurements presented here only represent lake breezes in July 2013; the same measurements taken in other months or years may show even more variability due to differences in meteorological conditions.

Some of our key findings include:

- Thermodynamic changes were large across the LBF, with dew points increasing by 2.5 °C on average and temperatures decreasing by 0.5 °C on average over distances ranging from 50 to 800 m. This creates a sharp thermodynamic gradient in the vicinity of the LBF.
- Each LBF was marked by a narrow area of convergence, with wind speeds generally 1 $m\ s^{-1}$ greater on average within the lake-breeze onshore flow.
- Lake-breeze circulations varied in depth both spatially and temporally. The depth of onshore flow ranged from 100 to 700 m on both lidar and rawinsonde measurements, with significant variability between cases and over the life cycle of the lake breeze. One out of five lake-modified airmass soundings showed thermodynamic changes associated with the lake breeze extending to 1000 m, higher than the depth of the onshore flow.
- Vertical velocities within the leading edge of the LBF ranged between 1–2 $m\ s^{-1}$ based on lidar measurements, velocities in thermal updrafts ahead of the LBF ranged from 2–3 $m\ s^{-1}$, and generally downward vertical velocities were recorded behind the LBF.
- Radar fine lines were found to correspond with the LBF locations during AMMOS transects.

The results from the ELBOW-MB project agree well with previous studies of LBFs in other locations and also demonstrate that both the thermodynamic and kinematic properties of the LBF and lake-breeze circulation can vary considerably both spatially and temporally over time. Further, these results provide forecasters in southern Manitoba with increased confidence when forecasting the impacts of lake-breeze circulations, especially in data sparse areas. Further investigation into the characteristics and variability of small lake LBFs using high-resolution data (eg. radiometer, rawinsonde, lidar, AMMOS), in particular in the context of the effects on convective initiation and development, is still needed.

Acknowledgments The authors would like to thank the Natural Sciences and Engineering Research Council (NSERC) for support of this research through a NSERC Discovery Grant to Hanesiak and NSERC undergraduate and graduate funding to Curry. We also thank the Canada Foundation for Innovation (CFI) for funding the AMMOS and lidar acquisition and the University of Manitoba for funding to support the mobilization of the equipment. Logistical, in-kind and equipment assistance from Environment and Climate Change Canada and RainyDay Internet (especially Jeff Klause) are greatly appreciated during ELBOW-MB. We would also like to thank Dave Patrick and Jason Knight (ECCC) for their assistance with radar data processing, and all the participants of the ELBOW-MB field project.

References

Alexander LS (2012) Mesoscale boundaries and storm development in southwestern Ontario during ELBOW 2001. PhD dissertation. York University, 325 pp (Available from the Centre for Research in Earth and Space Science, York University, 4700 Keele St., Toronto, ON M3J 1P3, Canada)

Asefi-Najafabady S, Knupp K, Mecikalskim JR, Welch RM, Phillips D (2010) Ground-based measurements and dual-Doppler analysis of 3-D wind fields and atmospheric circulations induced by a meso-γ-scale inland lake. J Geophys Res 115:D23117

Azorin-Molina C, Connell BH, Baena-Calatrava R (2009) Sea-breeze convergence zones from AVHRR over the Iberian Mediterranean area and the Isle of Mallorca, Spain. J Appl Meteorol Climatol 48:2069–2085

Brook JR, Makar PA, Sills DML, Hayden K, McLaren R (2013) Exploring the nature of air quality over southwestern Ontario: main findings from the Border Air Quality and Meteorology Study. Atmos Chem Phys 13:10461–10482

Crosman ET, Horel JD (2012) Idealized large-eddy simulations of sea and lake breezes: sensitivity to lake diameter, heat flux and stability. Boundary-Layer Meteorol 137:1–29

Curry ME, Hanesiak J, Sills DML (2015) A radar based investigation of lake breezes in southern Manitoba, Canada. Atmos Ocean 53:237–250

Estoque MA, Gross J, Lai HW (1976) A lake breeze over southern Lake Ontario. Mon Weather Rev 104:386196

Iwai H, Murayama Y, Ishii S, Mizutani K, Ohno Y, Hashiguchi T (2011) Strong updraft at a sea-breeze front and associated vertical transport of near-surface dense aerosol observed by doppler lidar and ceilometer. Boundary-Layer Meteorol 141:117–142

King PWS, Leduc MJ, Sills DML, Donaldson NR, Hudak DR, Joe P, Murphy PB (2003) Lake breezes in southern Ontario and their relation to tornado climatology. Weather Forecast 18:795–807

Laird NF, Kristovich DAR, Liang XZ, Arrit RW, Labas K (2001) Lake Michigan lake breezes: climatology, local forcing, and synoptic environment. J Appl Meteorol 40:409–424

Lyons WA (1972) The climatology and prediction of the Chicago lake breeze. J Appl Meteorol 11:1259–1270

NOAA (2015) Great Lakes Statistics. Retrieved from http://www.coastwatch.glerl.noaa.gov

Oke TR (1978) Boundary layer climates, 2nd edn. Methuen and Co Ltd, London 435 pp

Pearce RP (1955) The calculation of a sea-breeze circulation in terms of the differential heating across the coastline. Q J R Meteorol Soc 81:351–381

Segal M, Leuthold M, Arritt RW, Anderson C, Shen J (1997) Small lake daytime breezes: some observational and conceptual evaluations. Bull Am Meteorol Soc 78:1135–1147

Sills DML (1998) Lake and land breezes in southwestern Ontario: observations, analyses and numerical modeling. PhD dissertation. York University, 338 pp. (Available from the Centre for Research in Earth and Space Science, York University, 4700 Keele St., Toronto, ON M3J 1P3, Canada)

Sills DML, Brook JR, Levy I, Makar PA, Zhang J, Taylor PA (2011) Lake breezes in the southern Great Lakes region and their influence during BAQS-Met 2007. Atmos Chem Phys 11:7955–7973

Simpson JE (1994) Sea breeze and local wind. Cambridge University Press, Cambridge, UK 34 pp

Straka JM, Rasmussen EN, Fredrickson SE (1995) A mobile mesonet for finescale meteorological observations. J Atmos Ocean Technol 13:921–936

Stull RB (1988) An introduction to boundary layer meteorology. Kluwer, Boston 666 pp

Suresh R (2007) Observation of sea breeze front and its induced convection over Chennai in southern peninsular India using Doppler weather radar. Pure Appl Geophys 164:1511–1525

Taylor NM, Sills DML, Hanesiak JM, Milbrandt JA, Smith CD (2011) The Understanding Severe Thunderstorms and Alberta Boundary Layers Experiment (UNSTABLE) 2008. Bull Am Meteorol Soc 92:739–763

Tsunematsu N, Iwai H, Ishii S, Murayama Y, Yasui M, Mizutani K (2009) The formation of sharp multi-layered wind structure over Tokyo associated with sea-breeze circulation. SOLA 5:1–4

Wilson JM, Schreiber WE (1986) Initiation of convective storms at radar-observed boundary-layer convergence lines. Mon Weather Rev 114:2516–2536

Wurman J, Doweel D, Richardson Y, Markowski P, Rasmussen E, Burgess D, Wicker L, Blusestien HB (2012) The second verification of the origins of rotation in tornadoes experiment: VORTEX 2. Bull Am Meteorol Soc 93:1147–1170